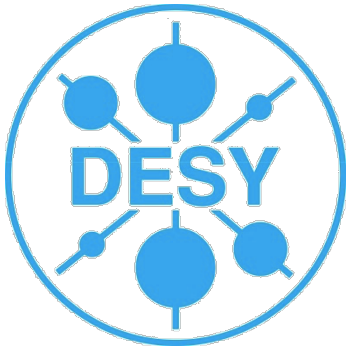

Study of lithium niobate crystals

Ekaterina Kochetkova
Lomonosov Moscow State University, Russia
DESY, Hamburg, Germany

September 5, 2017

Abstract

This report describes the study of the optical properties of lithium niobate crystals $LiNbO_3$. For this I used the analysis on the Lambda 1050 spectrometer and Varian 5000 spectrometer. Study of the optical properties of lithium niobate crystals, for optimize Optical to Terahertz conversion.

Supervisor: Dr. Nicholas Matlis

1. Introduction

1.1. General information on Lithium niobate

Lithium niobate ($LiNbO_3$; LN) is a unique photonic material and often referred to as the silicon of photonics. It has attracted a great deal of attention over the past three to four decades due to its favorable electro-optic, acousto-optics, non-linear optical properties, ease of fabrication, and robustness. It has generated interest over the years mainly due to its use in nonlinear optical frequency conversion, electro-optical modulation, surface acoustic wave devices, holographic data storage, optical waveguides, and integrated optical applications. In more recent times ferroelectric domain engineering of LN crystal has paved a new pathway for developing periodically poled $LiNbO_3$ (PPLN) for fabricating optical parametric oscillators (OPO) to generate tunable lasers in the visible and mid-infrared radiation ,tandem-poled lithium niobate crystals for the broadband green light source, laser projectors or display devices , and photonic band gap materials . Further, there is a considerable interest in micro-structuring of LN crystals for their use in the micro-electro-mechanical system (MEMS) [1]. Lithium niobate is used for THz generation in PPLN (participates in the creation multicycle THz) and bulk LN (participates in the creation single-cycle THz), which are necessary for work electron acceleration in AXSIS project. To optimization THz generation need to know optical properties of crystals LN.

Point Defects in $LiNbO_3$ crystals

Along with the inherent thermodynamically generated vacant sites, non-stoichiometry related Frankel defects i.e., Li vacancies V_{Li}^{-1} and Nb-antisites (Nb_{Li}^{5+}) are the main defects in congruent $LiNbO_3$ crystals. Li vacancies are the result of Li deficiency in the composition. The Nb-antisite is generated as the excess Nb of the CLN composition occupies the Li sites. Non-stoichiometry in $LiNbO_3$ arises due to the characteristic difference in its constitutional chemical bonds, i.e., Li–O and Nb–O bonds. The covalent Nb–O bonds are considerably stronger than the ionic Li–O bond. Due to the dissimilar bond strength and nearly equal ionic radii of the Li and Nb ions, there is a natural tendency of the available extra Nb ions to occupy the Li sites creating an antisite defect. Consequently, due to the charge difference in the Li^{+} and Nb^{5+} ions, additional Li vacancies appear in the $LiNbO_3$ lattice in order to maintain the charge neutrality.

Along with Li vacancies and Nb-antisites, there also exist oxygen vacancies (V_O^{2+}) and protons (H^{+}) in the form of OH and OD complexes. Being a transitional metal ion, Nb ions give rise to other defects such as free polaron (Nb_{Nb}^{4+}), bound polaron (Nb_{Li}^{4+}), and bi-polarons (Nb_{Li}^{4+}–Nb_{Li}^{4+}) by trapping electrons. Similarly, Li-vacancies also form hole-polarons by trapping holes. So, the departure from stoichiometry leads to a high degree of structural disorder and point defects in LN crystals.

In the literature there are three different models based on Li vacancies, Nb vacancies, and oxygen vacancies explaining the defect structure of LN. However, the most accepted model, explaining most of the properties of LN, is represented by the Li-site vacancy (V) model: $[Li_{1-5x}(Nb_{Li})_xV_{4x}][Nb][O_3]$ proposed by Larner et al.. According to this model the structure remains stable up to x = ~0.02 and the congruent melting is for x = 0.018. Figure 1 shows a representative model for the defect structure of CLN.

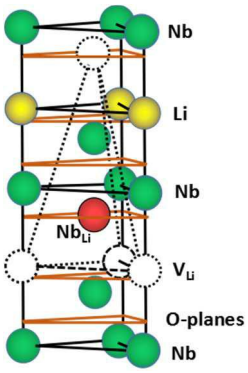

Figure 1. Schematic of the defect structure of a congruent $LiNbO_3$ crystal

Effect of Intrinsic Defect on Properties

It is well known that optical properties of a material are sensitive to the intrinsic defects and impurities. The $Nb_{Li}^{5+/4+}$ defects act as electron trap sites and form polaron (Nb_{Li}^{4+}) and bipolaron (Nb_{Li}^{4+}–Nb_{Li}^{4+}) states which are responsible for the photorefractive damage. The presence of these defects and impurities leads to light-induced changes in the refractive index that results in the optical distortion, phase modulation, Bragg scattering, and green induced infrared absorption (GIIRA), and consequently decreases the efficiency of nonlinear interactions when the crystal is subjected to an intense visible radiation. Because of these defects the value of the optical properties such as non-linear optical coefficient, linear electo-optic coefficient etc. (Table 1) is low in defect rich CLN crystal.

Table 1. A few properties of congruent lithium niobate (CLN) and near-stoichiometric lithium niobate (nSLN) crystals.

Parameter	CLN	nSLN
Li_2O:Nb_2O_5	48.6:51.4	49.9:50.1
Non-linear optical coefficient (pm/V) @ λ = 633 nm	d_{13} = 6.1 d_{33} = 34.1	d_{13} = 6.3 d_{33} = 44.0 (33% Higher)
Linear electo-optic coefficient (pm/V) @ λ = 1064 nm	r_{31} = 10.0 r_{33} = 31.5	r_{31} = 10.4 r_{33} = 38.3 (22% Higher)
Coercive field (kV/mm) @ room temperature	~21	<4 (80% Lower)

However, these light induced optical effects in CLN can be minimized to a significant extent by operating the device at higher temperature (~180 °C) or by using defect controlled stoichiometric LN having lesser intrinsic defects and impurities.

1.2. Motivation

The AXIS project has two tasks. The first task is make large amounts of THz radiation to accelerate electrons and the second task is to make THz radiation, using nonlinear optical conversion (difference frequency generation) of optical lasers. To achieve a highly efficient conversion, we can be done using $LiNbO_3$ (LN have a high nonlinear coefficient). For optimal THz conversion efficiencies, use cryogenic temperatures of $LiNbO_3$ because THz absorption is reduced.

Within the framework of the summer school project, several main points were considered. The first is, that optimize Optical to Terahertz conversion, need to know the optical properties of $LiNbO_3$.

As part of my research, I studied the optical properties of LN, because it is necessary to know for optimize Optical to Terahertz conversion.

During the summer school I encountered several such problems

1. The absorption and reflection are sources of energy loss for the optical beam, causing lower efficiencies
2. Absorption of high energy lasers can lead to heating of $LiNbO_3$ which lowers efficiencies because high crystal temperatures cause higher THz absorption.

1.3. Equipment and experiment

1.3.1. Lambda 1050 Spectrometer

Each sample (size 2,5 cm × 2,5 cm × 0,03 cm Fig.3) was cleaned and then placed in spectrometer. The experiment was carried out in the range from 180 to 1000 nm with polarizer and un-polarizer. The experiment can be divided into two stages. The one included experiments with first sample in different modes. The second stage included un-polarizer experiment with first sample, but with used new lamp. The second sample (2) was not clean, so it was not investigated on a spectrometer.

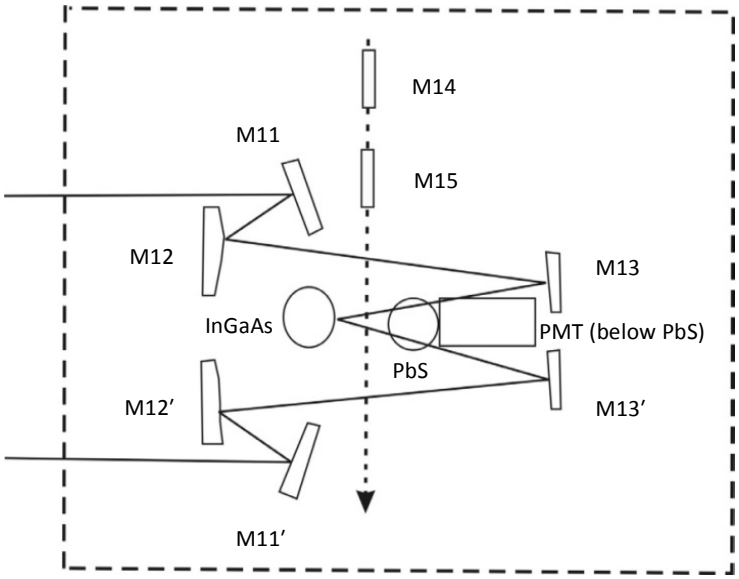

Figure 2. Optical system in the Lambda 1050 spectrometer detector compartment

The radiation passing alternately through the sample and reference beams is reflected by mirrors M11, M12, M13, and M11′, M12′, M13′, respectively of the optics in the detector assembly onto the appropriate detector.

Third, the detector compartment has the Three Detector Module fitted as standard. A photomultiplier tube (PMT) detector is used in the UV/Vis range (175–860 nm). In the NIR range you will have either a narrowband or a wideband InGaAs detector (860–1800 nm or 860–2500 nm, respectively) and a lead sulfide (PbS) detector (860–3300 nm) [2].

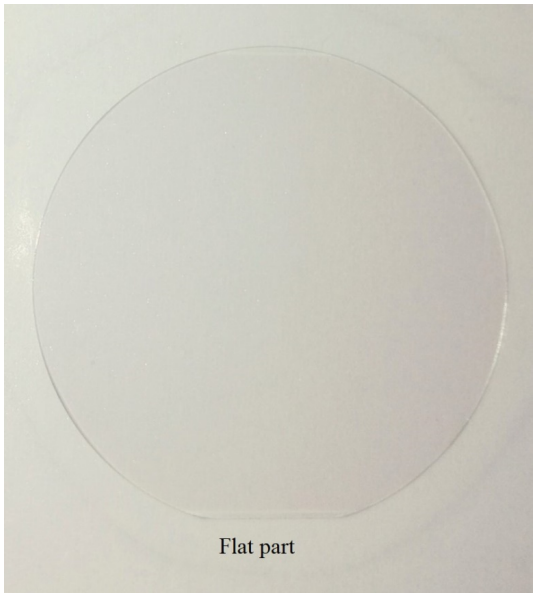

Figure 3. Lithium niobate sample

1.3.2. Varian 5000 Spectrometer

Each sample (Fig.3) was cleaned and then placed in spectrometer. The experiment was carried out in the range from 200 to 2500 nm polarizer and un-polarizer.

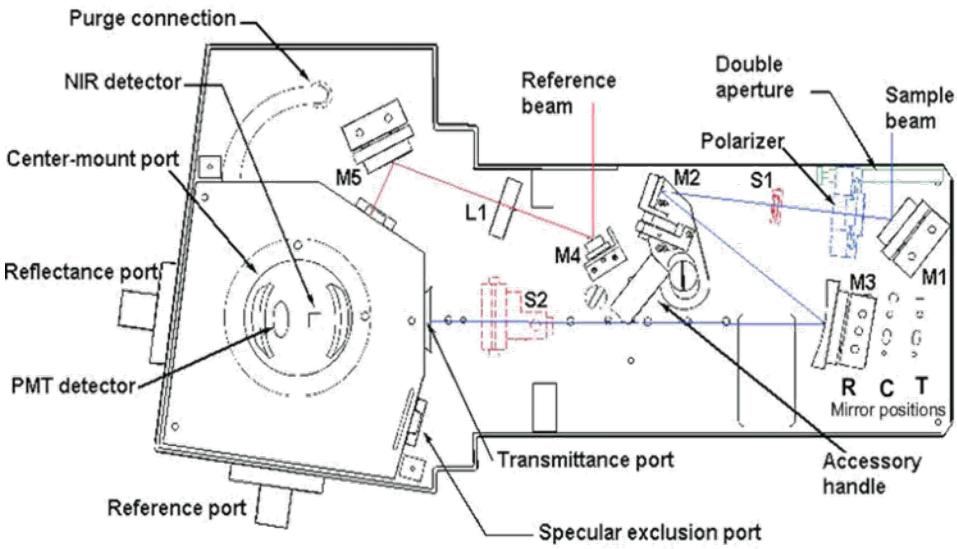

Figure 4. Diffuse Reflectance Accessory with beam path. [3]

2 Results

2.1. Results of the study on a Lambda 1050 Spectrometer

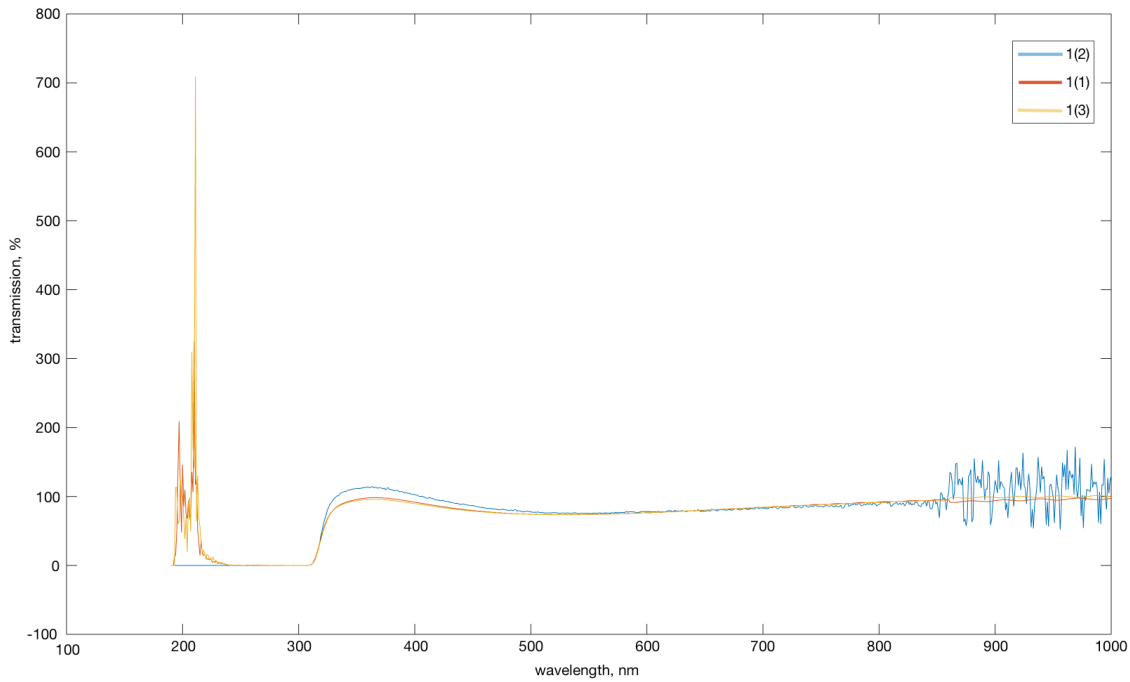

Figure 5.

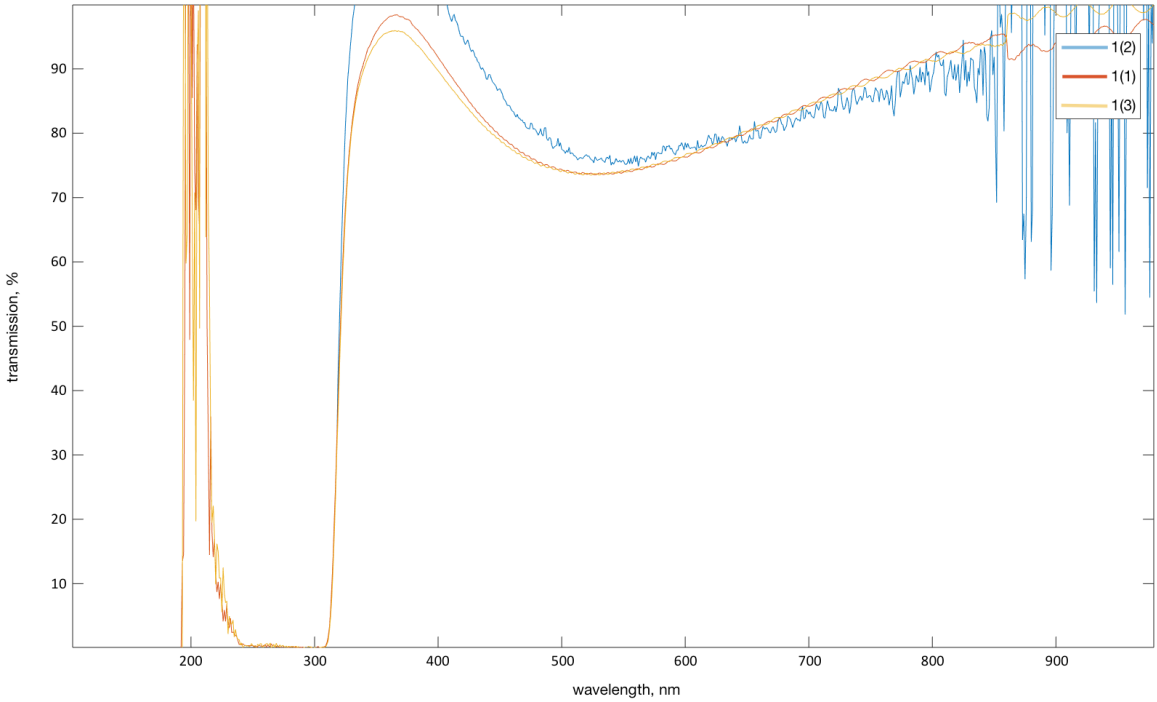

Figure 6.

Figure 5, 6 Spectra sample 1. 1(1) with 0 deg. pol., 1(2) un-pol. and 1(3) with 90 deg. pol..
Graphs 1(1), 1(2) and 1(3) were received in first stage and graph 1(4) was received in second stage of experiment.

Bandwidths in the range from 800 to 1000 nm are due to the capabilities of the lamp, because experiment 1(4) and 2 was performed using a new lamp to improve the quality of the spectrum. High transmission values in the range from 180 to 211 nm are explained by the possibility of measurement on this device for 1(4).

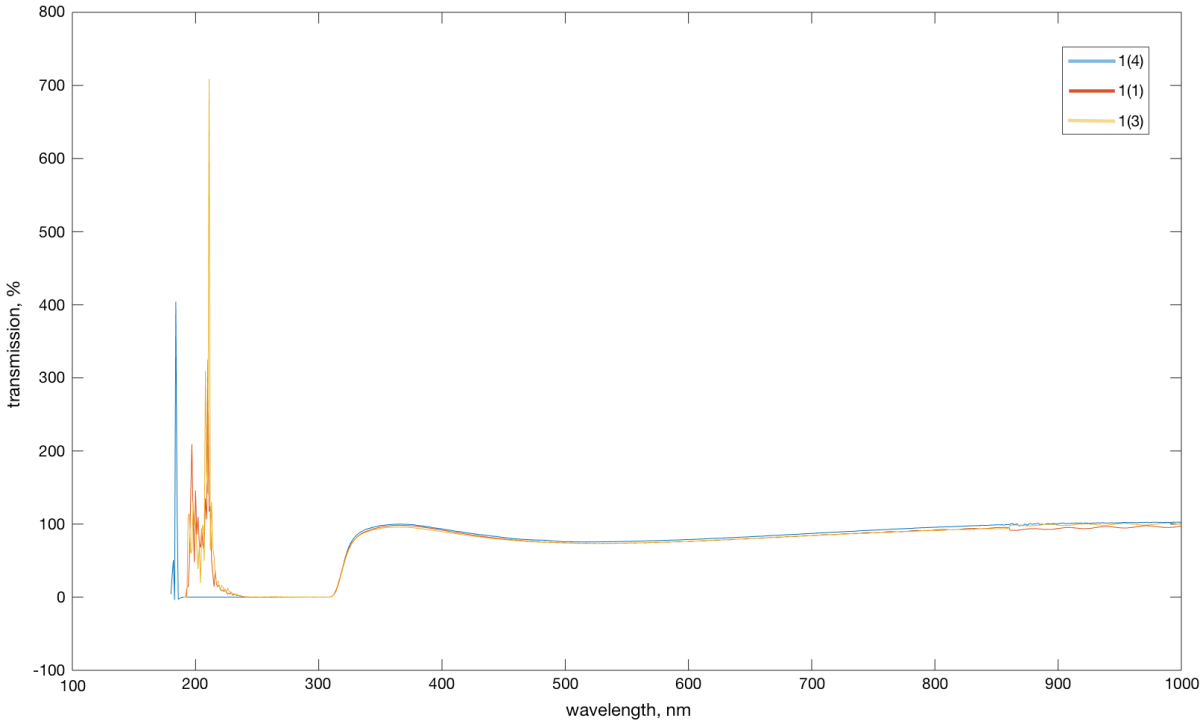

Figure 7.

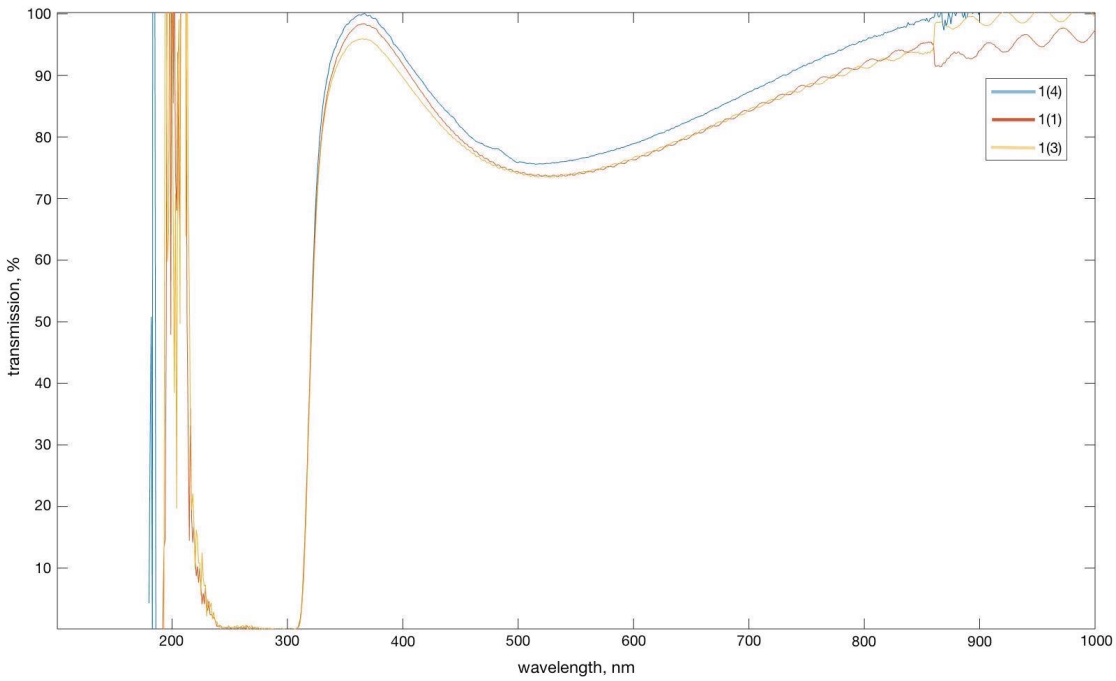

Figure 8.

Figure 7, 8 Spectra sample 1. 1(1) with 0 deg. pol., 1(3) with 90 deg. pol., and 1(4) with 0 deg. pol. new lamp.

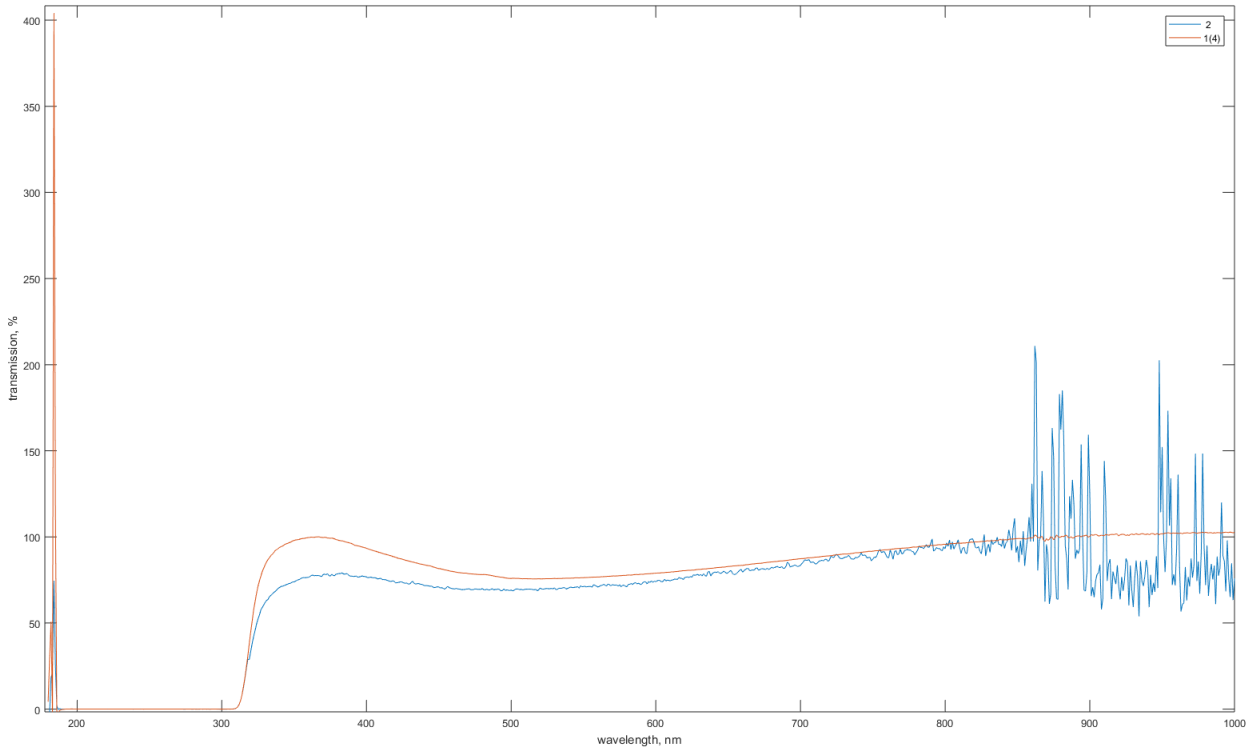

Figure 9 Spectra sample 1 (1(4) and sample 2 with 0 deg. pol. with new lamp

2.2. Results of the study on a Varian 5000 Spectrometer

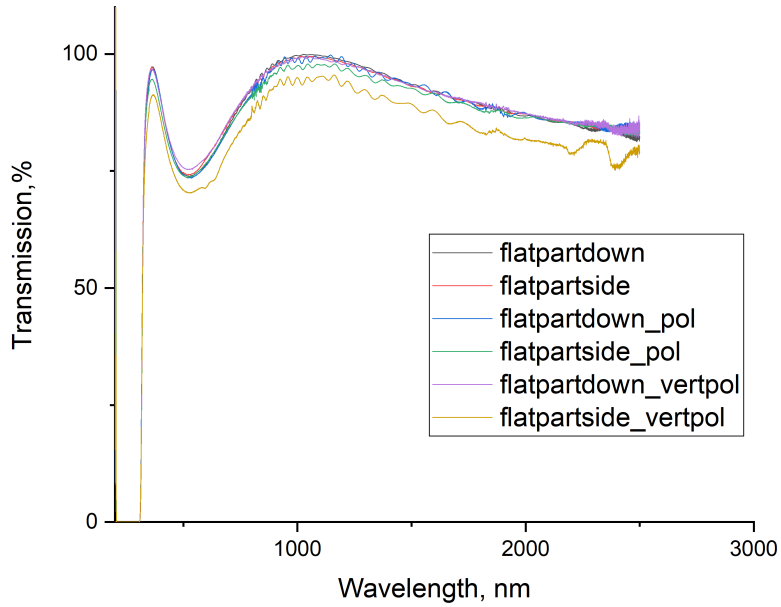

Figure 10. Spectra sample 1 un-pol. (Flatpartdown and Flatpartside), with 0 deg. Pol.(Flatpartdown_pol and Flatpartside_pol), with 90 deg. Pol. (Flatpartdown_vertpol and Flatpartside_vertpol)

The Fig.10 show the presence of a wide band about 520 nm for sample 1, this is typical for spectra un-pol and with 0 deg. pol, and 90 deg. pol. for differently oriented samples.The final transmission depends on absorption and on reflection. At transmission values close to 100%, I assumed that reflection is equal to 0. And to calculate the absorption I used formula:

A=100%-T%
Absorption (A)=0,2%

The spectra from the Varian 5000 spectrometer are similar to the spectra from the Lambda 1050 spectrometer, the transmission begins to increase at 305 nm. But when measured at Varian 5000 un-polarizer in the region from 800 to 1000 nm there is no excess there are no such jagged changes.

The Fig. 11 The graphs for sample 3 are similar in appearance to the absorption transmission graph, this similarity is shown in the Fig. 15.

This Fig.11 also shows the presence of a wide band about 516 nm for sample 4 and we see, that predict Reflection losses high transmission at 1030nm gives estimate of absorption at 1030 nm this samples have nearly 100% transmission at design wavelength of 1030 nm. But due to the fact that the transmission exceeds 100% (which is physically impossible), I could not calculate the absorption.

This Fig.12 shows the presence of a wide band about 511 nm, this typically for sample 3 and 4. Absorption for the third sample was 0.9%

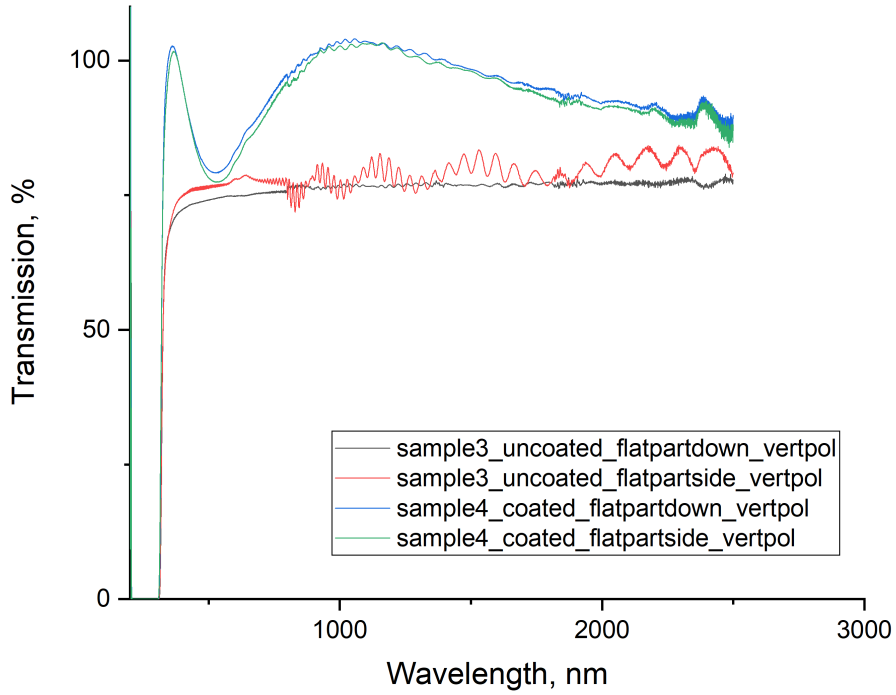

Figure 11. Spectra sample 3 and 4 with pol..

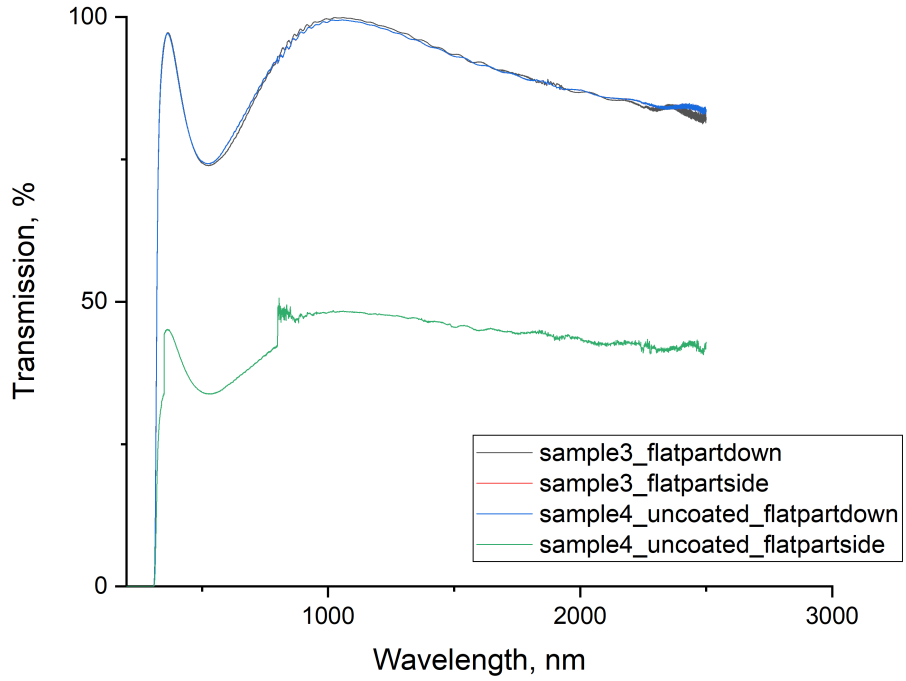

Figure 12. Spectra sample 3 and 4 un-pol..

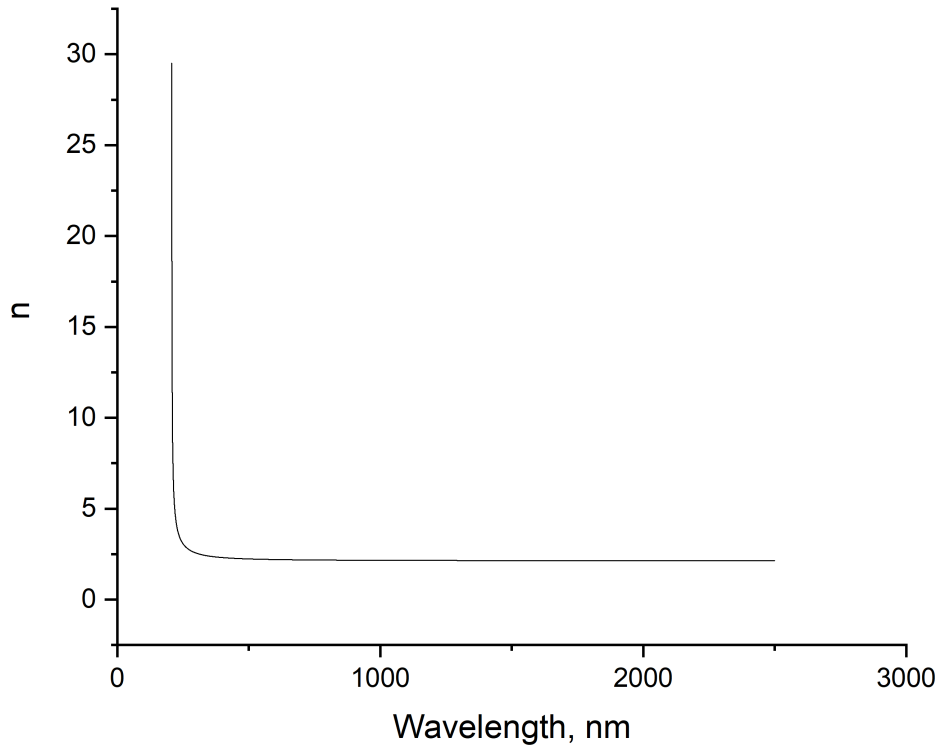

Figure 13. Dependence graph of refractive index on wavelength for LN

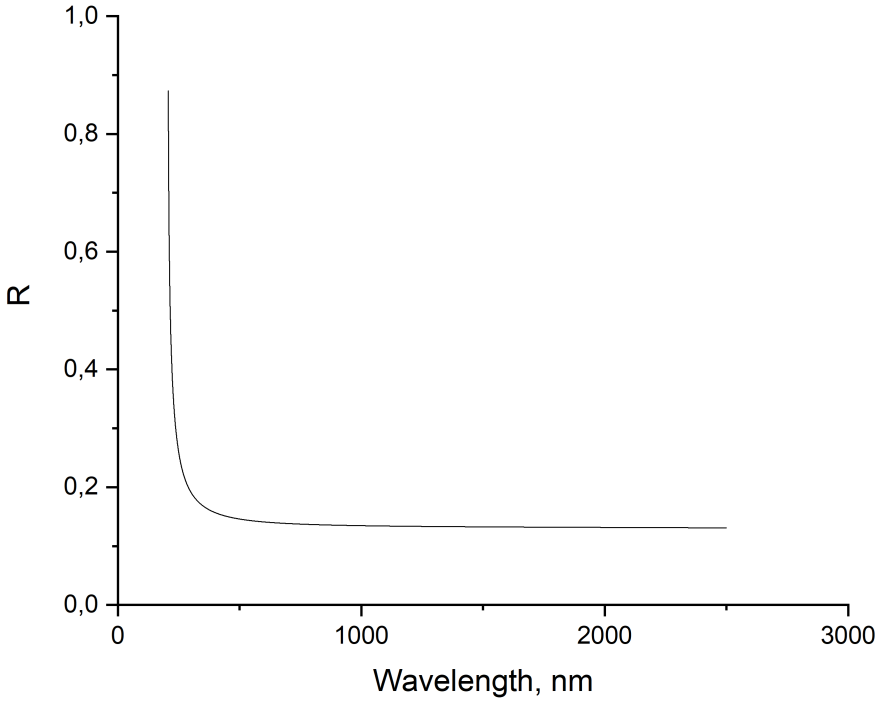

Figure 14. Dependence graph of reflectance on wavelength for LN

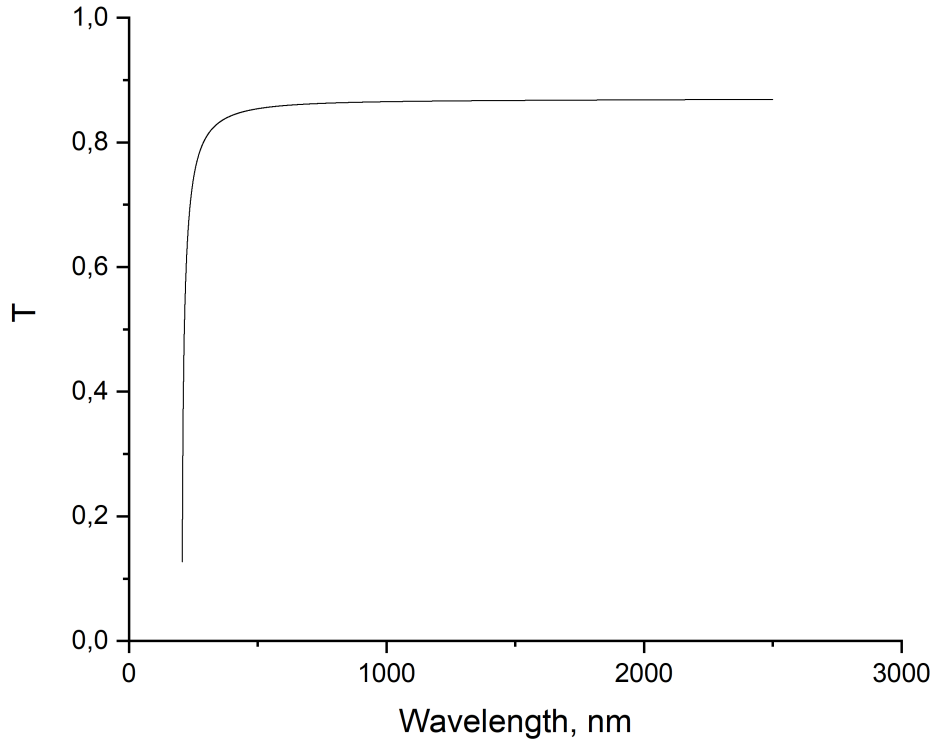

Figure 15. Dependence graph of transmission on wavelength for sample 3

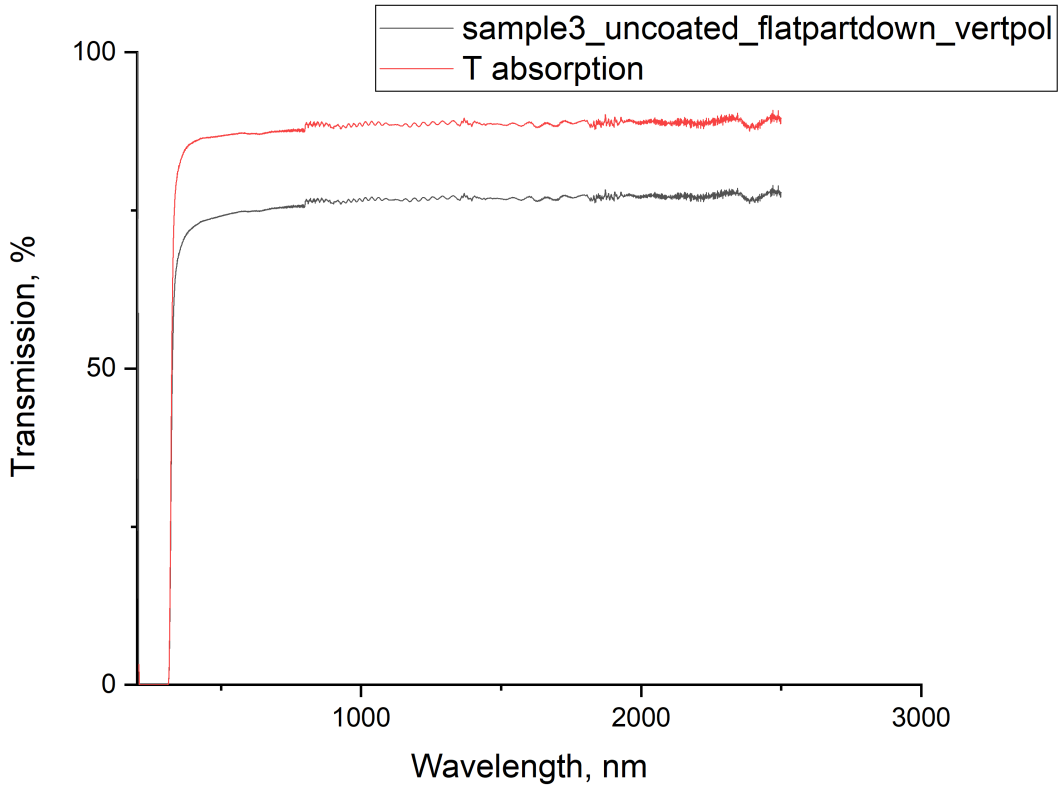

Figure 16. Dependence graph of transmission for sample 3 and transmission absorption on wavelength

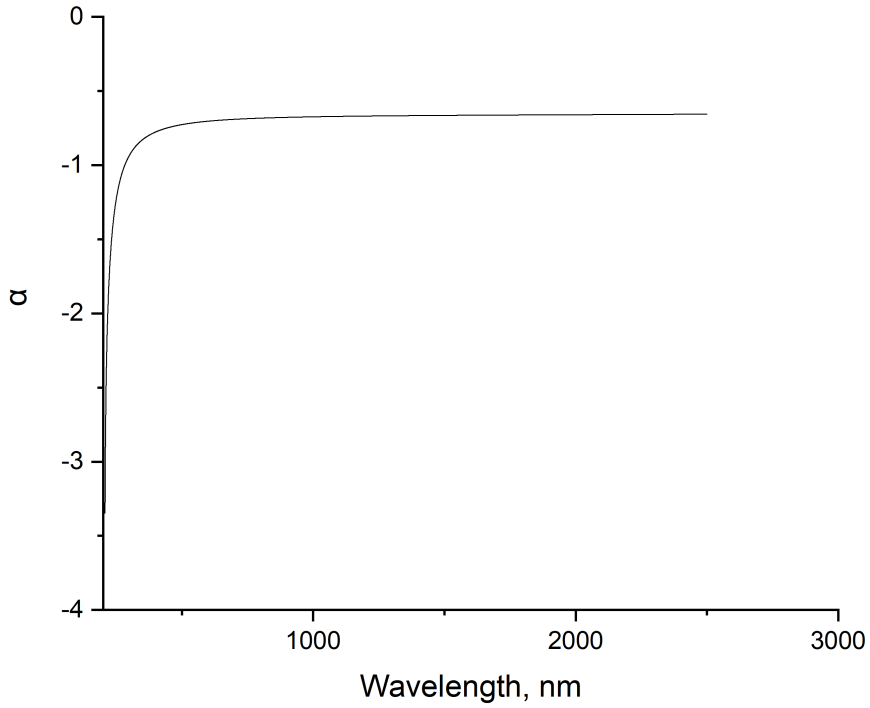

Figure 17. Dependence graph of absorption coefficient on wavelength for LN

$$n = \sqrt[2]{a_1 + b_1 * k + \frac{a_2 + b_2 * k}{\lambda^2 - (a_3 + b_3 * k)^2} + \frac{a_4 + b_4 * k}{\lambda^2 - {a_5}^2} - \frac{a_6}{\lambda^2}} \quad (1)$$

$$R = \frac{(1-n)^2}{(1+n)^2} \quad (2)$$

$$T = 1 - R \quad (3)$$

$$\alpha = \frac{1}{d} * (2*\log(1-R) - \ln(T) - \ln(1-(R^2)*e^{-2*0.1875*\alpha}) \quad (4)$$

d the thickness (d=0,1875), α the absorption coefficient

Using formulas (1), (2), (3),(4) which are taken from the article [4] it was possible to calculate the reflectance (R), refractive index (n), transmission (T), absorption coefficient (α) and construct graphs(Fig. 13,14,15,17). Absorption coefficient was calculated in MATLAB.

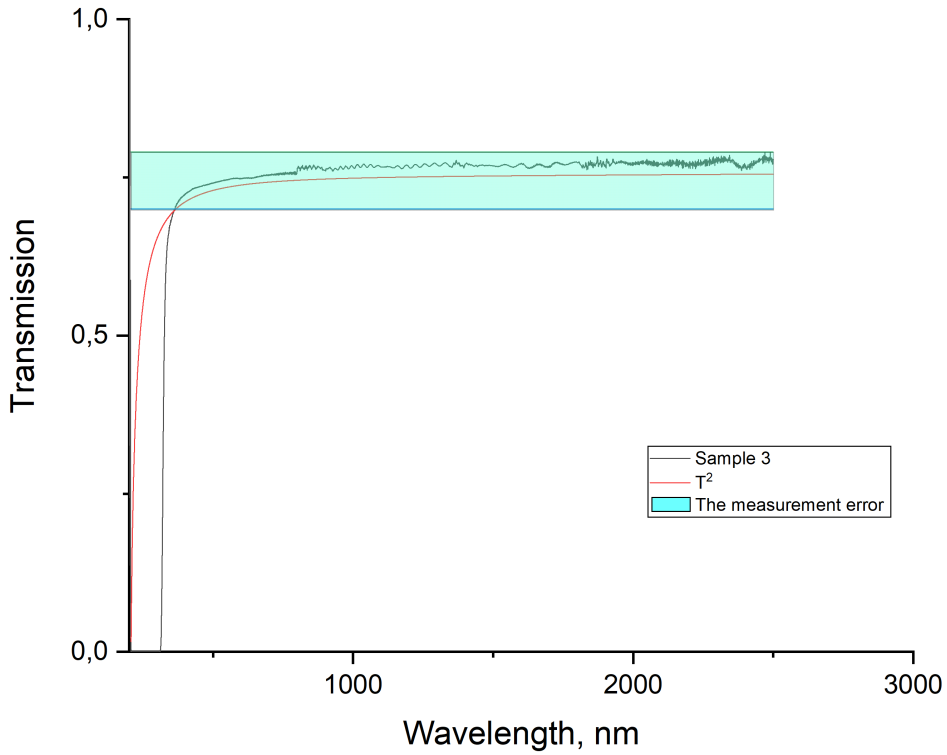

Figure 18. Spectra sample 3 and T^2 (square of the theoretically calculated transmission)

4. Conclusions

1. Transmission with coated samples at design wavelength of coating is near 100% this implies that optical absorption at this wavelength is very low.
2. If we compare the coated sample 1 and 2 (fig. 9), we can see that, unlike the first sample, the second sample has a serrated spectrum in the range from 800 to 1000 nm, even with a new lamp (for the first sample this problem was solved by replacing a lamp).
3. If we compare the coated (sample 3) and uncoated (sample 4) (fig. 11,12), we can see that, the transmission of the third sample is very high at about 1030 nm, the transmission of the entire graph is about 100%, while the fourth sample has a very low transmission (below 50%).
4. The measurement error was approximately 9%. In the course of my research, I was faced with the problem that the values of the transmission of sample 3 (uncoated sample) and square of the theoretically calculated transmission are very close to each other and the difference between the two values is less than the measurement error. Therefore, it was not possible to calculate the absorption with influence of value reflection for a given sample by formula $A = \frac{T\ sample}{T^2}$.

References

1. The optical damage resistance and absorption spectra of $LiNbO_3$:Hf crystals, Shuqi Li, China, 2006.
2. High-Performance Lambda Spectrometers, Hardware Guide, PerkinElmer, 2011.
3. Varian 5000 User Guide Manual, 2016.
4. Optical absorption properties of doped lithium niobate crystal, Zhu Jiangou, UK, 1991.